PERKIN 1

Boronic acid appended azo dyes–colour sensors for saccharides †

Christopher J. Ward,[a] Prakash Patel[b] and Tony D. James *[a]

[a] *Department of Chemistry, University of Bath, Claverton Down, Bath, UK BA2 7AY. E-mail: T.D.James@bath.ac.uk*
[b] *Avecia Ltd, Hexagon House, PO Box 42, Blackley, Manchester, UK M9 8ZS*

Received (in Cambridge, UK) 2nd October 2001, Accepted 7th December 2001
First published as an Advance Article on the web 21st January 2002

A number of boronic acid functionalised azo dye molecules have been prepared using a simple 3-step synthesis and their spectral properties upon complexation with monosaccharides investigated. The dyes undergo visible colour changes in aqueous solution upon addition of monosaccharide.

Introduction

A great amount of attention continues to be devoted to the development of synthetic molecular receptors with the ability to recognise neutral organic species, including saccharides.[1] The vast majority of these systems have relied upon hydrogen bonding interactions for the purposes of recognition and binding of guest species. However, there is still no designed, monomeric receptor that can compete effectively with bulk water for low concentrations of monosaccharide substrates.[2] As the chemistry of saccharides and related molecular species plays a significant role in the metabolic pathways of living organisms, detecting the presence and concentration of biologically important sugars in aqueous solution is necessary in a variety of medicinal and industrial contexts. The recognition of D-glucose is of particular interest, since the breakdown of glucose transport in humans has been correlated with certain diseases: renal glycosuria, cystic fibrosis, diabetes and also human cancer. Recent research provides clear evidence that tight control of blood sugar levels in diabetics sharply reduces the risk of long term complications, which include blindness, kidney failure, heart attacks and gangrene. Industrial applications range from the monitoring of fermentation processes to establishing the enantiomeric purity of synthetic drugs.[3]

The boronic acid–saccharide interaction can be utilised to overcome the problem of undesired solvent competition for the host. Boronic acids readily and reversibly form cyclic boronate esters with diols in aqueous basic media.[3] Saccharides contain a linked array of hydroxy groups that provide an ideal structural framework for binding to boronic acids. The most common interaction is with 1,2- and 1,3-diols of saccharides to form five- or six-membered rings respectively, *via* two covalent bonds (Scheme 1).

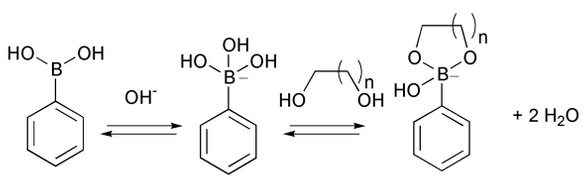

Scheme 1 Benzeneboronic acid complexation with diols

Lorand and Edwards determined the first stability trends and selectivities of various polyols and saccharides towards benzeneboronic acid.[4] The complex stability was shown to increase from ethylene glycol to D-fructose, *i.e.* from the simple acyclic diols to the rigid *cis*-diols of saccharides. This observed selectivity order has since been shown to be common to all monoboronic acids, not just benzeneboronic acid.[1] The suitability of the boronic acid functionality as a receptor for saccharides has been well established in fluorescence, circular dichroism and electrochemical studies.[1,3,5,6]

A fairly recent development has been the study of the effect of saccharides on the colour of dyes containing the boronic acid functionality. Boronic acid azo dyes have been known for over forty years where they were used for investigations in the treatment of cancer by the technique of Boron Neutron Capture Therapy (BNCT).[7–9] However, it has only been in the last decade that related dyes and their interaction with saccharides have been explored.

Nagasaki *et al.* observed that chromophores containing boronic acid moieties that aggregate in water, changed colour and deaggregated upon addition of saccharides.[10] This was rationalised by the boronic acid–saccharide complexation increasing the hydrophilicity of the bound species. Takeuchi *et al.* have prepared a boronic acid dye that undergoes an absorption spectral change on addition of nucleosides through binding of boronic acid to the ribose unit of the nucleosides.[11] Strongin has prepared a tetraboronic acid resorcinarene system **1** for the visual sensing of saccharides.[12] However, for a colour change to be observed the saccharide must be heated to 90 °C in DMSO. This reaction is irreversible so cannot be applied as a sensor system.

In 1994 Sandanayake and Shinkai reported 'the first known synthetic molecular colour sensor for saccharides'.[13] This designed molecular internal charge transfer (ICT) sensor **2** is based on the intramolecular interaction between the tertiary amine and the boronic acid group. The electron-rich amine creates a basic environment around the electron-deficient boron centre that has the effect of inducing the boronic acid–saccharide interaction and reducing the working pH of the sensor.[14] The electronic change associated with this decrease in the pK_a of the boronic acid moiety on saccharide complexation was shown to be transmitted to the neighbouring amine. This creates a spectral change in the connected ICT chromophore, which can be detected spectrophotometrically. The pK_a value associated with the boron–nitrogen interaction shifted on saccharide addition. More recently, Shinkai's group have synthesised a bis(boronic acid)-based saccharide receptor, bearing a photo-responsive azobenzene group which has shown high glucose selectivity when the azobenzene unit is switched to the thermodynamically unfavourable *cis* conformation.[15] They have also demonstrated that azobenzene derivatives bearing one or two aminomethylbenzeneboronic acid groups can be useful for practical colorimetric saccharide sensing in 'neutral' aqueous media.[16] Shinkai has applied the boronic acid–amine inter-

† Electronic supplementary information (ESI) available: absorption–pH titrations and absorption–saccharide titrations. See http://www.rsc.org/suppdata/p1/b1/b108896c/

 DOI: 10.1039/b108896c

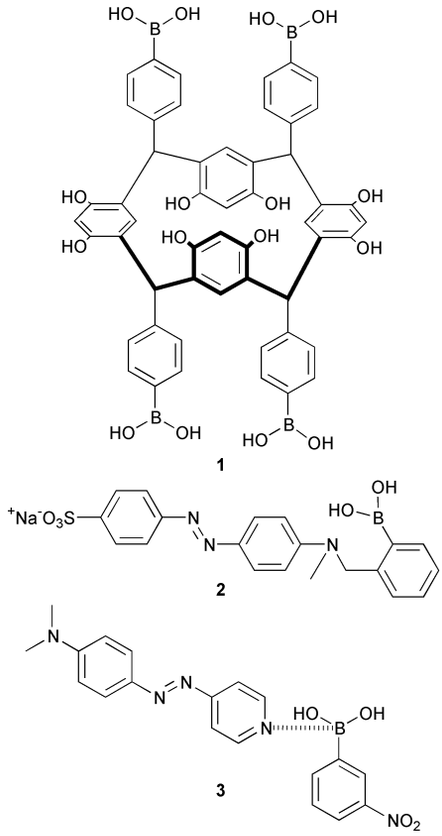

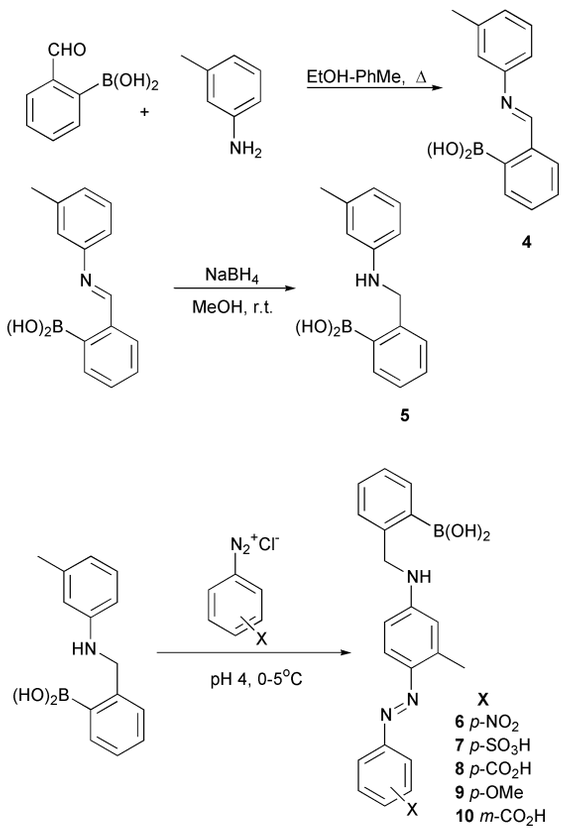

Scheme 2 Synthesis of boronic acid azo dyes.

action to the molecular design of a visualized intermolecular sensing system for saccharides.[17] 3-Nitrobenzeneboronic acid interacts with the pyridine nitrogen of 4-(4-dimethylaminophenylazo)pyridine **3** in methanol and changes its colour from yellow to orange. Added saccharides form complexes with the boronic acid and enhance the acidity of the boronic acid group. As a result, the boron–nitrogen interaction becomes stronger and the intensified intramolecular charge-transfer band changes the solution colour to red.

The main drawback in the development of coloured boronic acid–saccharide sensors, so far, has been the relatively small shifts achieved in the absorption bands of the chromophores upon saccharide binding. The aim of this research was to develop molecular ICT sensors, which would produce significant visible colour changes upon saccharide interaction. Furthermore, by changing the substituent on the azo group's aromatic ring to a variety of electron donating or withdrawing groups (*e.g.* methoxy or nitro groups), the electronics of the chromophore will be subtly altered. No study has been conducted on the effect of these substituents on saccharide binding with boronic acid azo dyes. If a system with a large colour change can be developed it could be incorporated into a diagnostic test paper for D-glucose, similar to universal indicator paper for pH. Such a system would make it possible to rapidly measure D-glucose concentrations without the need for specialist instrumentation. This would be of particular benefit to diabetics in developing countries.

Results and discussion

A. Synthesis of boronic acid azo dyes

We report herein a novel and facile synthetic route to boronic acid azo dyes, with little or no need for purification (Scheme 2). Commercial 2-formylbenzeneboronic acid is reacted with *m*-toluidine to form the respective imine. This is then reduced to the amine using a standard sodium borohydride reduction. The final step is to couple with the diazonium salt of a series of anilinic molecules (*e.g.* 4-nitroaniline) under normal diazotisation conditions to yield the boronic acid azo dyes as single isomers.

The reaction of *m*-toluidine with 2-formylbenzeneboronic acid was performed in a refluxing ethanol–toluene mix (10 : 1 v/v), with azeotropic removal of water by a Dean–Stark trap. The reaction works very well (isolated yield >90%) and always shows 100% conversion to imine **4** by proton NMR, so there is no need for any purification. The imine was reduced by an excess of sodium borohydride in dry methanol at room temperature. After an aqueous acidic work-up, amine **5** was obtained in good yield (81%) and excellent purity.

The final step was to perform the azo coupling reaction. These reactions occur predominately *para* to the electron-donating anilinic nitrogen because of steric effects, but *ortho* substitution can also be observed. However, it is known that by incorporating a methyl group *meta* to the anilinic nitrogen in the amine coupling agent, exclusive *para* coupling is observed.[18] Hence the inclusion of this design motif in the target dyes avoids potentially difficult separation of isomers. Azo coupling reactions were performed using the diazonium salts of 4-nitroaniline, sulfanilic acid (4-aminosulfonic acid), 4-aminobenzoic acid, *p*-anisidine (4-methoxyaniline) and 3-aminobenzoic acid, to yield the respective dyes **6**, **7**, **8**, **9** and **10**. A methanol–water solvent system was employed in all of the coupling reactions for solubility reasons. All dyes have been fully characterised.

This route is synthetically simpler than previously reported procedures. For example, Shinkai's route involved a moderately yielding lithiation reaction to make the boronic acid, followed by an azo coupling step that afforded two isomers that required separation and purification.[13]

B. UV–VIS studies

Ultraviolet–Visible (UV–VIS) spectrophotometry was used to study the boronic acid azo dye molecules' interaction with saccharides. The absorption of visible light by azo compounds can be described through a Linear Combination of Atomic Orbitals-Molecular Orbital (LCAO-MO) approach.[19] A non-bonding (n) electron from the azo nitrogen is excited, by the

absorption of a photon of visible light, into the lowest antibonding (π*) orbital in an n⟶π* electronic transition. The energy, and hence wavelength, of this transition is dependent upon the substituents of the azo chromophore and the inductive and conjugation effects that these have on the energy of the n and π* orbitals.

The anilinic nitrogen found in the target molecules is in conjugation with the azo nitrogens through the phenyl ring system. The anilinic nitrogen is also in close proximity to the boronic acid boron centre. The electronic changes associated with saccharide binding can be transmitted through a boron–anilinic nitrogen interaction to the azo chromophore, hopefully creating a spectral change in the molecule that can be detected in the UV–VIS absorption spectrum. It is well known that these electronic changes are often manifested in a pK_a change and it is this that can be studied by an UV–VIS absorption–pH titration.[13]

C. Absorption–pH titrations

Absorption–pH titrations, from pH 2 to 12, of each of the boronic acid azo dyes in 0.05 mol dm^{-3} NaCl in methanol–water (1 : 2, w/w), were followed using a UV–VIS spectrometer. The experiments were then repeated with 0.05 mol dm^{-3} D-fructose also present. The sodium chloride present acts as an "osmotic buffer" because small amounts of sodium chloride are formed on adjustment of the pH with sodium hydroxide and hydrochloric acid. Because the titrations are carried out in a methanol–water mixture rather than simply water, the measurement of pH using a standard electrode is not strictly applicable to this situation. However, De Ligny and Rehbach have shown that for solutions in 50% methanol the pH is only changed by 0.1 of a pH unit compared to a 100% water solution.[20] At percentages lower than 84% methanol, the error does not exceed 0.2 pH units, but for higher percentages it dramatically increases and for absolute methanol it is equal to 2 pH units.

Fig. 1 shows the absorption–pH profile of dye **10**. Fig. 2 shows the same experiment with the presence of 0.05 mol dm^{-3} D-fructose. D-Fructose was chosen as the test saccharide as past studies have shown that it gives the largest pK_a shifts on binding to mono-boronic acids compared to other monosaccharides.[4]

Fig. 3 is a plot of absorbance *versus* pH at 450 nm of dye **10** with and without D-fructose. This observed pK_a shift upon addition of saccharide is believed to be caused by the association of the boronic acid with the anilinic nitrogen.[13] The plot clearly shows a shift in this equilibrium upon addition of D-fructose. The spectra and absorbance–pH plots for all of the other dyes can be found in the Supplementary Information. †

The pK_a of this interaction can be calculated from the above data by using eqn. (1).

$$A = (A_0 + A_{lim}K_a[H^+])/(1 + K_a[H^+])^{21,22} \qquad (1)$$

A is the absorbance for a particular concentration of proton; A_0 is the initial absorbance; A_{lim} is the limiting (final) absorbance; K_a is the acid dissociation constant; [H$^+$] is the concentration of protons.

The pK_a curves were analysed in KaleidaGraph‡ using non-linear (Levenberg–Marquardt algorithm) curve fitting of eqn. (1).

The errors reported are the standard errors ($\pm\sigma/\sqrt{N}$) obtained from the best fit. The calculation was performed for all dyes with and without D-fructose. The results of these calculations are summarised in Table 1.

The results show that the applied equation is valid for calculating the pK_as of the dyes as the r^2 values show an excellent fit

‡ KaleidaGraph Version 3.51 for PC, published by Synergy Software and developed by Abelbeck Software, 2457 Perikiomen Avenue, Reading, PA 19606. A user defined curve fit [1 + $m2$ $m1$ ($M0$)]/[1 + $m1$ ($M0$)] derived from eqns (1) and (2) was used in all calculations. The initial value of $m1$ (K) was set to 1 and the initial value of $m2$ (A_{lim}) was set to 1.1. The variable ($M0$) was [H$^+$] for eqn. (1) and [guest] for eqn. (2). The allowable error was set to 0.001%. For all curves the coefficient of determination (r^2) was >0.98.

Table 1 Calculated pK_a values for all dyes with and without D-fructose

	Without D-fructose		With D-fructose		
Dye	pK_a	r^2	pK_a	r^2	ΔpK_a
6	10.19 ± 0.03	0.997	7.04 ± 0.04	0.998	3.15
7	10.01 ± 0.02	0.999	7.13 ± 0.03	0.998	2.88
8	9.93 ± 0.03	0.997	7.24 ± 0.04	0.995	2.69
9	10.22 ± 0.01	0.999	7.17 ± 0.02	0.999	3.05
10	10.07 ± 0.02	0.999	7.21 ± 0.04	0.996	2.86
13	9.68 ± 0.02	0.998	6.99 ± 0.04	0.996	2.69

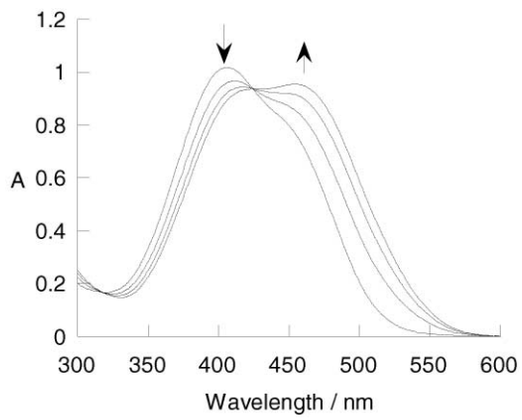

Fig. 1 Absorption–pH spectral changes of dye **10** (5.34 × 10^{-5} mol dm^{-3}). Representative spectra at pH = 6.59, 9.94, 10.49 and 10.97.

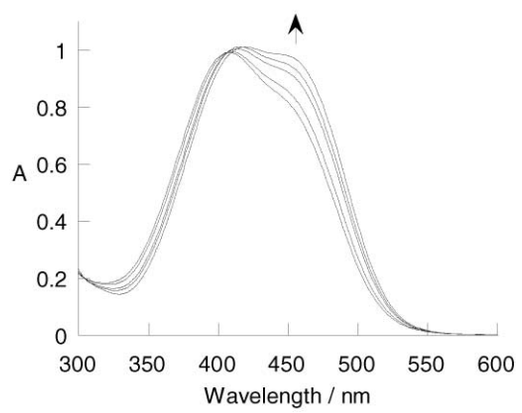

Fig. 2 Absorption–pH spectral changes of dye **10** (5.34 × 10^{-5} mol dm^{-3}) with 0.05 mol dm^{-3} D-fructose. Representative spectra at pH = 6.56, 7.01, 7.46, 7.98 and 10.99.

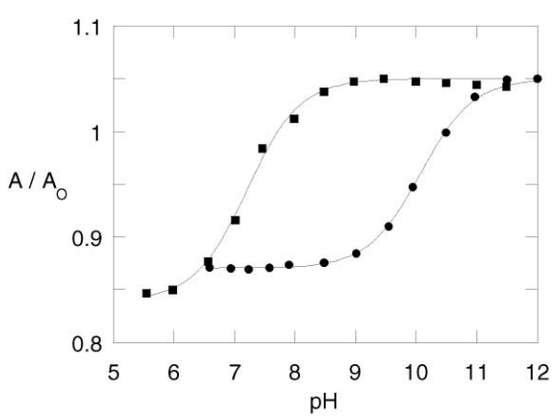

Fig. 3 Absorption–pH profile of dye **10** with and without D-fructose at 450 nm. (■) With no D-fructose, (●) with 0.05 mol dm^{-3} D-fructose.

($r^2 > 0.99$). This shift on saccharide binding (ΔpK_a) is in agreement with previous work and can be explained by the decrease in boron–oxygen bond angle upon saccharide binding, which increases the acidity of the boron centre.[4] All of the dyes show similar magnitudes of ΔpK_a, although dye **6** shows the largest change.

All of the dyes gave similar absorption spectra to dye **10**, with and without D-fructose. However, dye **6** (derived from 4-nitroaniline) showed an especially marked difference in its absorption spectra at high pH (Fig. 4 and Fig. 5).

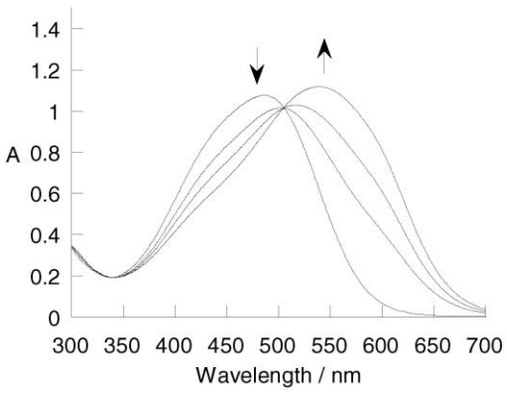

Fig. 4 Absorption–pH spectral changes of dye **6** (5.66×10^{-5} mol dm^{-3}). Representative spectra at pH = 8.05, 9.93, 10.46 and 10.98.

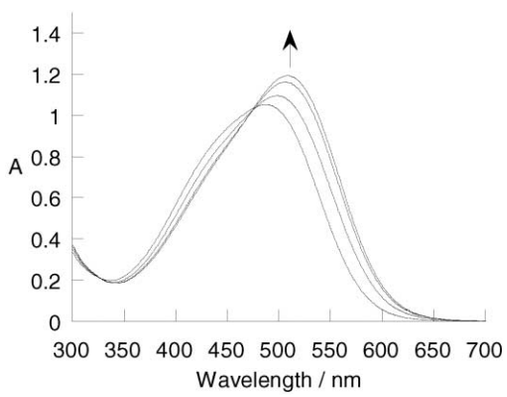

Fig. 5 Absorption–pH spectral changes of dye **6** (5.66×10^{-5} mol dm^{-3}) with 0.05 mol dm^{-3} D-fructose. Representative spectra at pH = 5.09, 7.03, 8.00 and 10.97.

D. Absorption–saccharide titrations

Fig. 5 shows that at high pH, in the presence of D-fructose, that dye **6**'s absorption maxima do not shift to as long a wavelength as without saccharide. This is actually a large enough shift (55 nm) to give a visible colour change from dark purple to red, upon the binding of D-fructose. To investigate this phenomenon further it was decided to perform a D-fructose titration with dye **6** in pH 11.32 aqueous methanolic buffer solution [52.1 wt% methanol (KCl, 0.01000 mol dm^{-3}; $NaHCO_3$, 0.002771 mol dm^{-3}; Na_2CO_3, 0.002771 mol dm^{-3})].[23]

This same colour change was observed. The experiment was repeated with D-glucose and ethylene glycol. The colour–absorbance changes upon addition of D-glucose to **6** are shown in Fig. 6 and the absorption spectra of this titration are shown in Fig. 7.

In all three cases there is a maximum wavelength shift of approximately 55 nm upon complexation. The concentration of the guest required to produce the change is different in each case, which is due to the different stability constants of the binding species. The wavelength shift obtained upon addition of saccharide with dye **6** is the largest achieved to date in such a system.

D-Fructose and D-glucose titrations at pH 11.32 were also performed on the other dyes. Although all showed colour

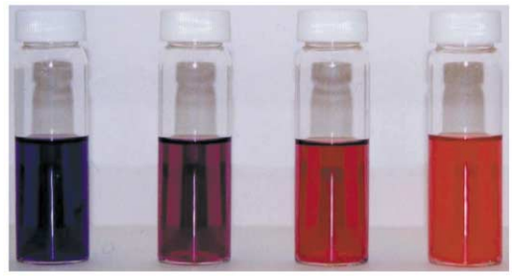

Fig. 6 Colour–absorbance changes upon addition of D-glucose to dye **6** (5.66×10^{-5} mol dm^{-3}); from left to right: with no saccharide, with 0.339×10^{-2} mol dm^{-3} D-glucose, with 1.66×10^{-2} mol dm^{-3} D-glucose and with 22.7×10^{-2} mol dm^{-3} D-glucose.

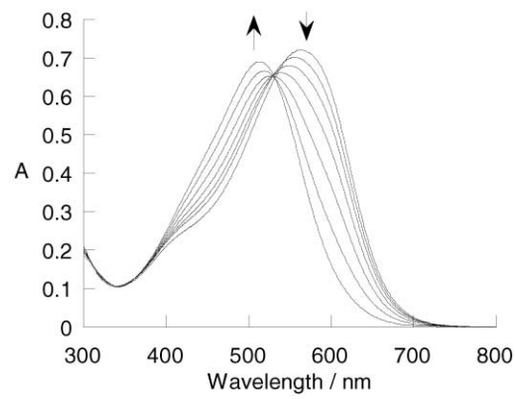

Fig. 7 Absorption spectral changes of dye **6** (2.83×10^{-5} mol dm^{-3}) with increasing concentration of D-glucose at pH 11.32. Representative spectra at [D-glucose] = 0, 1.69, 3.51, 7.06, 14.2, 28.4 and 56.8×10^{-3} mol dm^{-3}.

changes upon saccharide binding, none gave as large a spectral shift as dye **6**. The stability constants (K) of the boronic acid dye–saccharide complexes can be calculated using eqn. (2).

$$A = (A_0 + A_{lim} K [guest])/(1 + K [guest])^{21,22} \qquad (2)$$

A is the absorbance for a particular concentration of guest; A_0 is the initial absorbance; A_{lim} is the limiting (final) absorbance; K is the stability constant of the receptor with the guest; [guest] is the concentration of the guest.

The stability constant curves were analysed in KaleidaGraph ‡ using non-linear (Levenberg–Marquardt algorithm) curve fitting of eqn. (2). The errors reported are the standard errors ($\pm\sigma/\sqrt{N}$) obtained from the best fit.

Fig. 8 shows the curve fit using eqn. (2) for dye **6**'s interaction

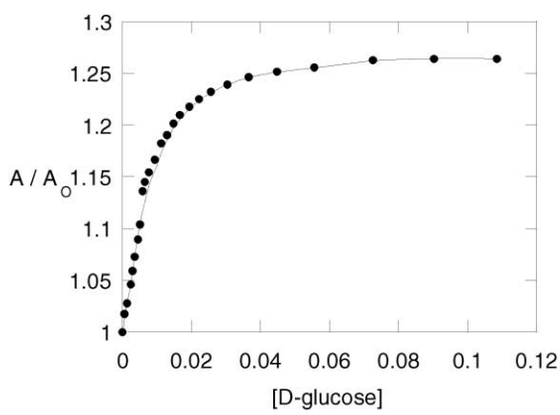

Fig. 8 Curve fit to determine the stability constant of dye **6** with D-glucose at 509 nm.

with D-glucose. Table 2 gives the results of these calculations for all of the boronic acid azo dyes.

The results show that dye **6**, which gives the largest spectral

Table 2 Stability constants (K) for polyol–boronic acid azo dye complexes at pH 11.32

Dye	Polyol	K	r^2	σ-value[a]
6	D-Fructose	2550 ± 250	0.991	0.78
6	D-Glucose	123 ± 9	0.983	0.78
6	Ethylene glycol	5.1 ± 0.1	0.999	0.78
7	D-Fructose	3630 ± 274	0.995	0.38[b]
7	D-Glucose	184 ± 40	0.982	0.38[b]
8	D-Fructose	4160 ± 352	0.992	0.13[c]
8	D-Glucose	121 ± 9	0.997	0.13[c]
9	D-Fructose	5180 ± 229	0.998	−0.27
9	D-Glucose	163 ± 16	0.993	−0.27
10	D-Fructose	5590 ± 201	0.999	0.10[c]
10	D-Glucose	198 ± 20	0.993	0.10[c]
13	D-Fructose	—[d]	—	0.78
13	D-Glucose	—[d]	—	0.78

[a] See ref. [25]. [b] Value for SO_3^-. [c] Value for CO_2^-. [d] Could not be determined from absorbance data.

change, has the lowest binding constant with D-fructose, compared to the other dyes. If a comparison is made to the relevant Hammett σ-values for the phenylazo-ring substituents, a trend is apparent for the *para*-substituted dyes. The binding constant is seen to increase as the σ-value becomes less positive, *i.e.* the ring substituent becomes less electron-withdrawing. Dye **10** shows the highest binding constant. Dye **10** is the only *meta*-substituted dye in the series and, as such, will have an inductive effect on the chromophoric system, rather than the conjugative resonance influence of the *para*-substituted dyes.

E. Proposed equilibria

At intermediate pH values Shinkai proposes that a boron–nitrogen interaction is prevalent, whereas at high and low pH this bond is broken.[13] What makes dye **6**'s equilibria more interesting is the presence of the anilinic hydrogen, which gives rise to different species at high pH. This apparently simple modification in the molecular structure seems to be responsible for the enhanced response of these dyes relative to those previously reported. Scheme 3 shows the proposed equilibrium species for dye **6** responsible for the observed colour change, consistent with the experimental results to date.

In the absence of saccharide, at pH 11.32, the observed colour is purple and in the presence of saccharide the colour is red (Fig. 6). From previous work it is known that when saccharides form cyclic boronate esters with boronic acids, the Lewis acidity of the boronic acid is enhanced and therefore the Lewis acid–base interaction between the boronic acid and the amine is strengthened.[1,6] This stronger B–N interaction will favour the red species over the equivalent saccharide bound purple species. The reason for this can be understood by considering species **W** and **X** from Scheme 3. In the presence of saccharide the B–N interaction in species **X** is stronger than that in species **W**. The increased B–N interaction of species **X** will make the N–H proton of species **X** more acidic than the corresponding bond in species **W**. Therefore, at higher pH species **X** will deprotonate to form the red species **Z**, whereas the weaker B–N bond in species **W** is broken by hydroxide ion to form the purple coloured species **Y**.

The colour change arises from the different electronic environment of the anilinic nitrogen. As mentioned earlier, the anilinic nitrogen is conjugated to the azo chromophore. A change in the environment of this nitrogen leads to changes in the energy levels of the n and π* orbitals of the azo chromophore and hence to a change in the absorption energy and wavelength. The proposal of these equilibrium species may also explain why Shinkai's dye did not give a visible spectral shift on saccharide binding. Because the anilinic nitrogen is tertiary in nature rather than secondary, there is no possibility of deprotonation, so the high pH boron–nitrogen bond cannot be

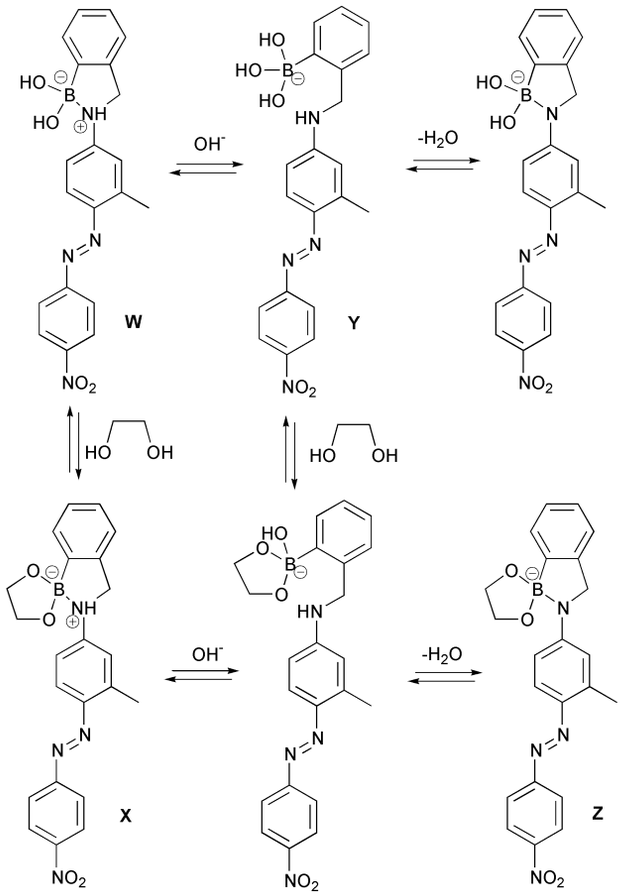

Scheme 3 Equilibria species.

formed. Hence there is no differentiation between the equilibrium species at high pH and consequently no spectral shift is observed.

F. Further evidence of proposed equilibria species

It must be stressed again that the equilibria discussed here for dye **6** are only proposals that fit the current experimental data. It was decided to use Electrospray Ionisation Mass Spectrometry (ESIMS) to see if any of the proposed equilibrium species could be observed. The fructose-bound high pH red species (**Z** in Scheme 3) was indeed detected (m/z 533) by negative ion ESIMS.

If removal of the anilinic proton in the saccharide-bound high pH species is the key to the spectral change, then replacing this proton with an alkyl group should prevent this phenomenom from occurring. It was decided to synthesise the *N*-methylated derivative of the nitro-substituted boronic acid azo dye to try to prove this hypothesis. The synthetic route to dye **13** is outlined in Scheme 4. Model dye **15** (with no boronic acid binding site) was also synthesised, for comparison purposes, using the route shown in Scheme 1 starting from benzaldehyde rather than 2-formylbenzeneboronic acid.

N-Methyl-*m*-toluidine was reacted with 1-bromo-2-bromomethylbenzene to form the tertiary amine **11**. This was lithiated and then reacted with trimethylborate to generate boronic acid **12**, after an acidic work-up. Coupling of **12** with the diazonium salt of 4-nitroaniline, as before, afforded the *N*-methylated boronic acid azo dye molecule **13**. The overall yield for the reaction sequence was below average. However, the route has not been optimised in any way.

The previously performed pH and saccharide titrations were repeated with dyes **13** and **15**. Unfortunately, dye **15** showed solubility problems in the aqueous environment used for the titrations, but, as expected, showed no spectral changes upon addition of saccharide under these conditions. The absorption

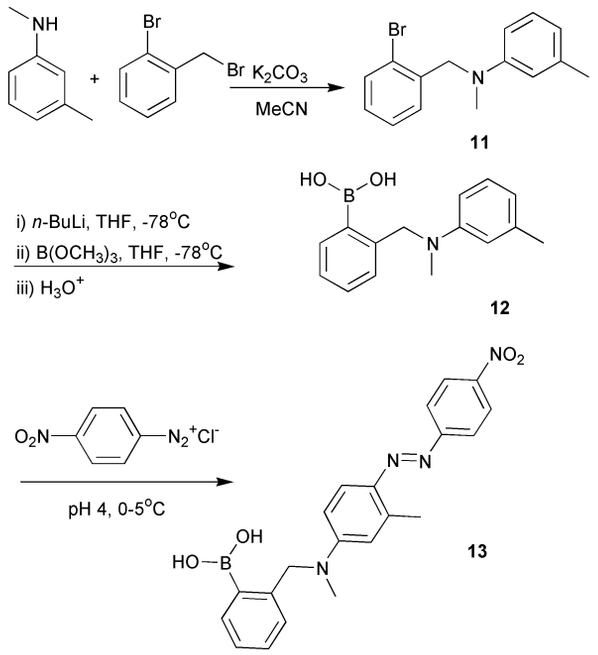

Scheme 4 Synthesis of *N*-methylated boronic acid azo dye.

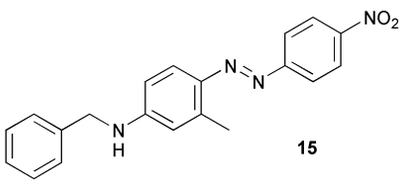

spectra of the D-fructose titration at pH 11.32 with **13** are shown in Fig. 9.

In this case, there is no shift in the wavelength upon saccharide complexation, only a small increase in the intensity of absorption. Consequently dye **13** does ***not*** change colour with added saccharide. The anilinic nitrogen of **13** is tertiary in nature, rather than secondary as in the case of **6**, so there is no possibility of deprotonation from this nitrogen. Consequently,

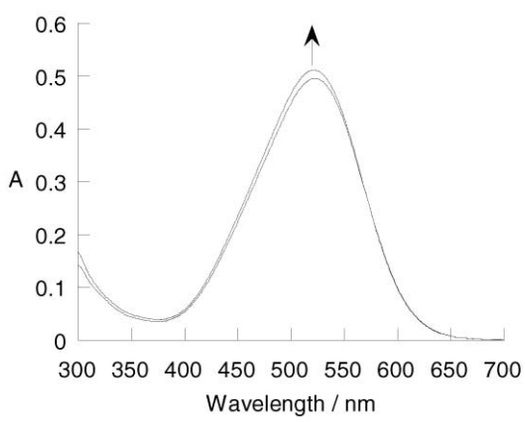

Fig. 9 Absorption spectral changes of dye **13** with increasing concentration of D-fructose at pH 11.32. Representative spectra at [D-fructose = 0 and 55.6 × 10^{-3} mol dm^{-3}.

the high pH B–N bond cannot form and there can be no electronic differentiation between the high pH saccharide bound species and the unbound species. Hence no colour change is observed.

It was decided to carry out some saccharide titrations at near neutral pH to investigate further the effect of pH on the equilibria. UV–VIS absorbance titrations of dyes **6** and **13** with D-fructose and D-glucose were performed in a pH 8.21 aqueous methanolic buffer solution [52.1wt% methanol (KCl, 0.01000 mol dm^{-3}; KH_2PO_4, 0.002752 mol dm^{-3}; Na_2HPO_4, 0.002757 mol dm^{-3})].[23] The pH of the buffer was chosen so that it was below the pK_a's of the unbound dyes, which are typically around 10 (Table 1). This should mean that, at the beginning of the titrations, the major solution dye species should be that containing the boron–nitrogen interaction. Fig. 10 and Fig. 11

Table 3 Stability constants (*K*) for polyol–boronic acid azo dye complexes at pH 8.21.

Dye	Polyol	K/dm^3 mol^{-1}	r^2
6	D-Fructose	291 ± 24	0.994
6	D-Glucose	26 ± 6	0.981
13	D-Fructose	371 ± 7	0.999
13	D-Glucose	23 ± 1	0.998

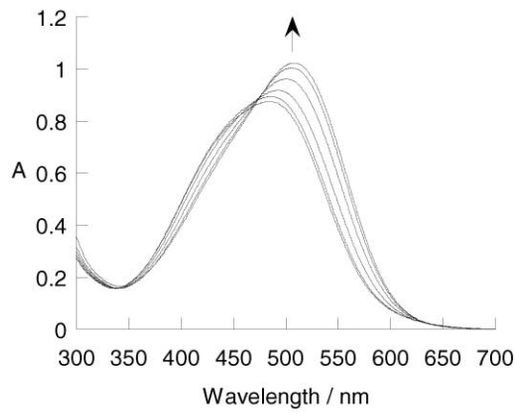

Fig. 10 Absorption spectral changes of dye **6** (2.83 × 10^{-5} mol dm^{-3}) with increasing concentration of D-fructose at pH 8.21. Representative spectra at [D-fructose] = 0, 0.23, 1.97, 7.17, 28.5 and 113 × 10^{-3} mol dm^{-3}.

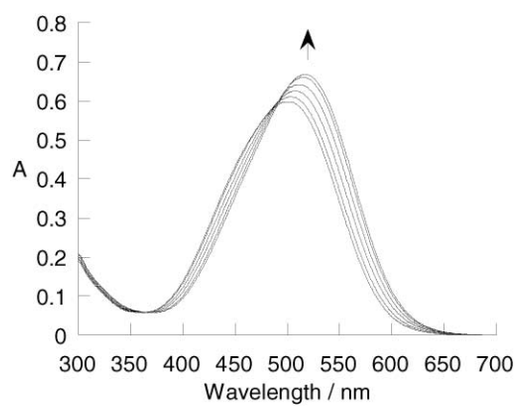

Fig. 11 Absorption spectral changes of dye **13** (2.00 × 10^{-5} mol dm^{-3}) with increasing concentration of D-fructose at pH 8.21. Representative spectra at [D-fructose] = 0, 1.10, 2.50, 5.63, 15.8 and 112 × 10^{-3} mol dm^{-3}.

show the respective absorption–spectral changes for the titrations with D-fructose. In both cases, as the concentration of saccharide was increased, a spectral shift to longer wavelength was observed. The shifts, and subsequent colour changes were not as pronounced (< 20 nm) as the high pH titrations with dyes **6**–**10**.

The stability constants (*K*) of the boronic acid dye–saccharide complexes can again be calculated using eqn. (2), assuming a 1 : 1 boronic acid–saccharide binding event. Table 3 shows the results of these calculations for the two dyes. An interesting point to note about the stability constants at pH 8.21 (Table 3) is that they are approximately a factor of ten smaller than those at pH 11.32 (Table 2). It is known that stability constants measured at near neutral pH are lower than the corresponding anionic stability constants at higher pH.[24]

Dye **6**'s spectral shift at pH 8.21 is in the opposite direction to that seen at pH 11.32. What is apparent from this titration is that when dye **6** is complexed to saccharide, it does not matter what the starting pH is, the final solution saccharide-bound species is always the same, with an absorbance maximum at 509 nm. In contrast, dye **13** has only one high pH species, no matter if it is saccharide-bound or not. As saccharide is added to dye **13** at pH 8.21, it must form the tetrahedral boronate anionic species. This is shown in Fig. 9 and Fig. 11 for dye **13**, where the absorbance maximum of the saccharide bound species is at 521 nm in both instances.

Conclusions

The development of a facile and clean synthesis of boronic acid azo dyes has been achieved. The boronic acid azo dyes show visible colour change upon saccharide complexation. The absorbance maximum of boronic acid azo dye **6** shifts by 55 nm to shorter wavelength upon addition of diols at high pH–the largest observed to date in such a system. Comparison with *N*-methylated dye **13** confirms that removal of the anilinic nitrogen proton in **6**, when bound with saccharide, gives rise to the pronounced colour change.

Experimental

^{1}H and ^{13}C NMR spectra were recorded on Bruker AC-300 and Bruker AC-400 spectrometers. All spectral data are reported relative to tetramethylsilane as the internal standard using the δ scale. The multiplicities of the spectroscopic data are presented in the following manner: s-singlet, d-doublet, m-multiplet, t-triplet, br-broad. *J*-values are given in Hertz. Due to quadrapolar relaxation, the aryl carbon atoms attached directly to the boronic acid boron atoms are not observed by ^{13}C NMR.

Infrared spectra were recorded on a Perkin–Elmer Paragon 1000 FT-IR spectrometer and a Perkin–Elmer 1600 Series FT-IR spectrometer. Samples were run either as a Nujol mull or as pressed KBr disks.

Electron Impact (EI) mass spectra were recorded on a VG ProSpec mass spectrometer. Liquid Secondary Ion (LSI) mass spectra were recorded on a VG ZabSpec instrument. A Micromass LCT mass spectrometer was used for Electrospray Ionisation (ESI) mass spectra. Fast Atom Bombardment (FAB) and EI mass spectra were also recorded on a double focussing, magnetic sector Micromass Autospec instrument, using a DEC Alpha data system running Opus V3.4X software, overlaid on an Open VMS operating system. High Resolution Mass Spectra (HRMS) were obtained from all of the above instruments.

Elemental analyses were performed at the University of North London, the University of Birmingham and the University of Bath. Melting points were measured on Gallenkamp and Büchi 535 melting point apparatus and are uncorrected.

UV–Visible absorption measurements used Sigma Spectrophotometer Silica (Quartz) Cuvets with 10 mm path lengths and were recorded on a Perkin–Elmer Lambda 20 UV/VIS Spectrophotometer. Data was collected *via* the Perkin–Elmer UV Winlab software package on a PC running Microsoft NT v4. All pH measurements were recorded on a Hanna Instruments HI 9321 Microprocessor pH Meter that was calibrated using Fisher Chemicals standard buffer solutions (pH 4.0–phthalate, 7.0–phosphate, and 10.0–borate).

Thin-layer chromatography (TLC) was performed on precoated aluminium-backed silica gel plates supplied by Merck Ltd. (Silica Gel 60 F_{254}, thickness 0.2 mm, Art. 5554). Visualisation was achieved by UV light (254 nm).

Acetonitrile was dried by refluxing with calcium hydride. It was subsequently distilled and collected by dry syringe as required. Prior to use, tetrahydrofuran and diethyl ether were distilled from sodium benzophenone ketyl under a nitrogen atmosphere. All other reagents and solvents were used as supplied by the Aldrich Chemical Co. Ltd., Lancaster Synthesis Ltd., Fisher Scientific Ltd., Acros Organics, Tokyo Kasei Kogyo (TCI) Co. Ltd., Merck Ltd. and Frontier Scientific Europe Ltd.

N-(2-Dihydroxyborylbenzylidene)-*m*-tolylamine (4)

m-Toluidine (0.72 g, 6.67 mmol) and 2-formylbenzeneboronic acid (1.00 g, 6.67 mmol) were mixed in absolute ethanol (45 ml) and toluene (5 ml). A Dean–Stark trap was fitted to permit the azeotropic removal of water, and the reaction mixture heated at reflux overnight (18 hours). After cooling, the solvent was removed *in vacuo* to obtain **4** (1.35 g, 92%) as a cream coloured solid: mp 170–172 °C (dec.); ν_{max}(Nujol)/cm^{-1} 1732 (CH=N); δ_H(300 MHz; CD_3OD; Me_4Si) 2.41 (3 H, s, Ar–CH_3), 7.24 (1 H, d, *J* 6.0, Ar–*H*), 7.34–7.46 (2 H, m, Ar–*H*), 7.51–7.66 (4 H, m, Ar–*H*), 7.70 (1 H, d, *J* 6.0, Ar–*H*), 9.12 (1 H, s, ArN=C*H*Ar); δ_C(75 MHz; CD_3OD; Me_4Si) 21.9, 120.3, 123.8, 129.6, 129.9, 130.9, 131.1, 131.5, 134.9, 135.1, 140.0, 141.1, 143.9, 166.6; *m*/*z* (LSIMS) 509 ([M − 2 H_2O + 2 NOBA]$^+$, 22%), 357 ([M + 1 NOBA − H_2O]$^+$, 100) and 222 ([M − H_2O]$^+$, 17).

N-(2-Dihydroxyborylbenzyl)-*m*-tolylamine (5)

Sodium borohydride (0.79 g, 20.9 mmol, 5 equiv.) was added slowly to **4** (1.00 g, 4.18 mmol) in dry methanol (50 ml). The reaction was left to stir at room temperature for 2 hours and then poured into ice–water (20 ml). Hydrochloric acid (1 M, 10 ml) was added slowly and the mixture left to stir for 30 minutes, whereupon the precipitate formed was collected by suction filtration to afford **5** (0.82 g, 81%) as a white solid (Found: C, 69.6; H, 6.4; N, 5.8. $C_{14}H_{16}BNO_2$ requires C, 69.7; H, 6.7; N, 5.8%); mp 72–73 °C (dec.); δ_H(300 MHz; CD_3OD; Me_4Si) 2.20 (3 H, s, Ar–CH_3), 4.29 (2 H, s, ArCH_2–NHAr), 6.54–6.66 (4 H, m, Ar–*H*), 6.99 (1 H, t, *J* 7.5, Ar–*H*), 7.15–7.32 (4 H, m, Ar–*H*); δ_C(75 MHz; CD_3OD; Me_4Si) 22.3, 52.2, 115.1, 118.6, 122.9, 127.1, 128.2, 130.0, 130.3, 133.0, 140.3, 146.1, 149.0; *m*/*z* (LSIMS) 241 ([M]$^+$, 40%), 223 ([M − H_2O]$^+$, 100).

N-(2-Dihydroxyborylbenzyl)-[3-methyl-4-(4-nitrophenylazo)-phenyl]amine (6)

4-Nitroaniline (0.10 g, 0.70 mmol) was mixed in water (1 ml), methanol (1 ml) and hydrochloric acid (1 ml, 5.0 M) and then cooled to 0–5 °C on an ice-bath. A chilled solution of sodium nitrite (0.06 g, 0.84 mmol, 0.2 M) was added dropwise. Excess nitrite was destroyed by the addition of sulfamic acid after stirring for 5 minutes. *N*-(2-Dihydroxyborylbenzyl)-*m*-tolylamine (0.16 g, 0.66 mmol) was dissolved in methanol (2 ml) and dilute hydrochloric acid (1 ml, 1 M) then added dropwise to the reaction mixture, which quickly turned a red colour. Sodium acetate was added to raise the pH of the solution to 4 and this was then left to stir at 0–5 °C for 3 hours. Sodium hydroxide (2 M) was slowly added to raise the pH to 7. The resulting precipitate was collected by suction filtration and dried in a dessicator overnight to afford **6** (0.19 g, 74%) as a dark red solid (HRMS: Found 372.1381, [M − H_2O]$^+$. $C_{20}H_{17}BN_4O_3$ requires 372.1392); mp 120–122 °C (dec.); λ_{max}(pH 8.05, 0.05 mol dm^{-3} NaCl, 33% MeOH: 67% H_2O w/w)/nm 486 (ε/dm^3 mol^{-1} cm^{-1} 19000); ν_{max}(KBr disk)/cm^{-1} 1602 (N=N), 1518 and 1333 (NO_2); δ_H(300 MHz; CD_3OD; Me_4Si) 2.63 (3 H, m, Ar–CH_3), 4.45 (2 H, s, ArCH_2–NHAr), 6.52–6.58 (1 H, m, Ar–*H*), 6.99–7.04 (1 H, m, Ar–*H*), 7.18–7.40 (5 H, m, Ar–*H*), 7.63–7.72 (1 H, m, Ar–*H*), 7.87–7.93 (1 H, m, Ar–*H*), 8.21–8.36 (2 H, m, Ar–*H*); δ_C(125 MHz; CD_3OD; Me_4Si) 18.1, 49.7, 113.2, 114.7, 118.3, 122.7, 123.6, 125.7, 127.6, 128.1, 129.8, 130.2, 132.8, 144.3; *m*/*z* (EI) 373 ([MH −H_2O]$^+$, 66%), 222 ([M − H_2O–$N_2C_6H_4NO_2$]$^+$, 100).

4-[4-(2-Dihydroxyborylbenzylamino)-2-methylphenylazo]-benzenesulfonic acid (7)

The above procedure was repeated with sulfanilic acid (0.08 g, 0.44 mmol) in place of *p*-anisidine (all other reagents were used in the same mole ratios), to afford **7** (0.05 g, 27%) as a dark red solid (HRMS: Found 424.1142, $[M - H]^+$. $C_{20}H_{19}BN_3O_5S$ requires 424.1138); mp 219 °C (dec.); λ_{max}(pH 8.18, 0.05 mol dm^{-3}NaCl, 33% MeOH: 67% H_2O w/w)/nm 421 (ε/dm^3 mol^{-1} cm^{-1} 19300); ν_{max}(KBr disk)/cm^{-1} 1610 (N=N), 1350 and 1150 (SO_2); δ_H(300 MHz; CD_3OD; Me_4Si) 2.59 (3 H, m, Ar–CH_3), 4.41 (2 H, s, ArCH_2–NHAr), 6.49–6.59 (2 H, m, Ar–*H*), 7.19–7.41 (4 H, m, Ar–*H*), 7.59–7.66 (1 H, m, Ar–*H*), 7.81 (2 H, d, *J* 9.0, Ar–*H*), 7.92 (2 H, d, *J* 9.0, Ar–*H*); δ_C(125 MHz; CD_3OD; Me_4Si) 18.0, 49.7, 113.1, 113.7, 115.1, 117.9, 122.9, 127.5, 127.9, 129.8, 132.7, 146.6, 153.7, 155.7; *m*/*z* (ESI) 424 ($[M - H]^+$, 33%), 406 ($[M - H_3O]^+$, 100).

4-[4-(2-Dihydroxyborylbenzylamino)-2-methylphenylazo]benzoic acid (8)

The above procedure was repeated using 4-aminobenzoic acid (0.11 g, 0.83 mmol) instead of 3-aminobenzoic acid (all other reagents were used in the same mole ratios), to afford **8** (0.10 g, 31%) as an orange–red solid (Found: C, 64.8; H, 5.0; N, 10.7. $C_{21}H_{20}BN_3O_4$ requires C, 64.8; H, 5.2; N, 10.8%); mp 208–210 °C (dec.); λ_{max}(pH 8.42, 0.05 mol dm^{-3} NaCl, 33% MeOH: 67% H_2O w/w)/nm 418 (ε/dm^3 mol^{-1} cm^{-1} 16000); ν_{max}(KBr disk)/cm^{-1} 1602 (N=N), 1684 (C=O); δ_H(300 MHz; CD_3OD; Me_4Si) 2.60 (3 H, m, Ar–CH_3), 4.42 (2 H, s, ArCH_2–NHAr), 6.50–6.61 (2 H, m, Ar–*H*), 7.18–7.41 (4 H, m, Ar–*H*), 7.61–7.68 (1 H, m, Ar–*H*), 7.82 (2 H, d, *J* 9.0 Ar–*H*), 8.11 (2 H, d, *J* 9.0 Ar–*H*); δ_C(125 MHz; CD_3OD; Me_4Si) 18.1, 49.6, 117.9, 122.8, 127.5, 131.6; *m*/*z* (LSIMS) 660 ($[MH - 2H_2O + 2$ NOBA$]^+$, 55%), 460 ($[M - 2H_2O + 2CH_3OH + K]^+$, 100).

***N*-(2-Dihydroxyborylbenzyl)-[4-(4-methoxyphenylazo)-3-methylphenyl]amine (9)**

The previous experiment was repeated using *p*-anisidine (0.61 g, 4.98 mmol, 6 equiv.) instead of 4-aminobenzoic acid. Purification was performed by washing the product (in dichloromethane) with 10% sodium hydrogen carbonate solution (w/w) to remove residual acetic acid, to yield **9** (0.11 g, 35%) as a orange–brown solid (Found: C, 67.3; H, 5.8; N, 10.2. $C_{21}H_{22}BN_3O_3$ requires C, 67.2; H, 5.9; N, 11.2%); mp 102–103 °C (dec.); λ_{max}(pH 8.42, 0.05 mol dm^{-3} NaCl, 33% MeOH: 67% H_2O w/w)/nm 400 (ε/dm^3 mol^{-1} cm^{-1} 14600); ν_{max}(KBr disk)/cm^{-1} 1602 (N=N); δ_H(300 MHz; CD_3OD; Me_4Si) 2.56 (3 H, m, Ar–CH_3), 3.84 (3 H, s, Ar–OCH_3), 4.39 (2 H, s, ArCH_2–NHAr), 6.49–6.59 (2 H, m, Ar–*H*), 7.00 (2 H, d, *J* 9.0, Ar–*H*), 7.20–7.40 (4 H, m, Ar–*H*), 7.52–7.57 (1 H, m, Ar–*H*), 7.76 (2 H, d, *J* 9.0, Ar–*H*); δ_C(125 MHz; CD_3OD; Me_4Si) 18.0, 49.7, 56.0, 113.8, 115.2, 115.5, 117.5, 124.8, 127.5, 127.8, 129.7, 132.6, 141.3, 144.3, 145.0, 149.0, 152.5, 162.5; *m*/*z* (ESI) 376 ($[MH]^+$, 100%).

3-[4-(2-Dihydroxyborylbenzylamino)-2-methylphenylazo]benzoic acid (10)

The previous experiment was repeated using 3-aminobenzoic acid (0.06 g, 0.41 mmol) instead of 4-nitroaniline (all other reagents were used in the same mole ratios), to yield **10** (0.10 g, 61%) as a red solid (Found: C, 64.9; H, 5.2; N, 10.9. $C_{21}H_{20}BN_3O_4$ requires C, 64.8; H, 5.2; N, 10.8%); mp 133–135 °C (dec.); λ_{max}(pH 8.48, 0.05 mol dm^{-3} NaCl, 33% MeOH: 67% H_2O w/w)/nm 406 (ε/dm^3 mol^{-1} cm^{-1} 19000); δ_{max}(KBr disk)/cm^{-1} 1603 (N=N); δ_H(300 MHz; CD_3OD; Me_4Si) 2.62 (3 H, m, Ar–CH_3), 4.40 (2 H, s, ArCH_2–NHAr), 6.50–6.60 (2 H, m, Ar–*H*), 7.18–7.42 (4 H, m, Ar–*H*), 7.52–7.66 (2 H, m, Ar–*H*), 7.94–8.05 (2 H, m, Ar–*H*), 8.37–8.41 (1 H, m, Ar–*H*); δ_C(125 MHz; CD_3OD; Me_4Si) 19.1, 52.5, 114.2, 118.9, 123.1, 125.4, 128.2, 128.6, 129.0, 130.8, 131.2, 132.2, 133.7, 133.7, 143.8, 145.1, 145.8, 154.6, 155.9, 170.9; *m*/*z* (ESI) 418 ($[MH - 2H_2O + 2CH_3OH]^+$, 100%).

***N*-(2-Bromobenzyl)-*N*-methyl-*m*-tolylamine (11)**

2-Bromobenzyl bromide (10.0 g, 40.0 mmol) was mixed in distilled acetonitrile (100 ml) with potassium carbonate (16.6 g, 120 mmol, 3 equiv.). The system was evacuated and put under an argon atmosphere. *N*-Methyl-*m*-toluidine (4.8 g, 40.0 mmol) was syringed into solution and the reaction mixture heated to reflux. After 4 hours, TLC analysis showed the reaction had gone to completion. The solvent was removed, after filtration, to yield **11** as a yellow oil (2.22 g, 98%); δ_H(300 MHz; $CDCl_3$; Me_4Si) 2.53 (3 H, m, Ar–CH_3), 3.19 (3 H, s, N-CH_3), 4.69 (2 H, s, ArCH_2–NMeAr), 6.60–6.72 (3 H, m, Ar–*H*), 7.19–7.39 (4 H, m, Ar–*H*), 7.67–7.71 (1 H, m, Ar–*H*); δ_C(125 MHz; $CDCl_3$; Me_4Si) 22.1, 38.8, 57.5, 109.3, 112.7, 117.7, 122.8, 127.6, 128.0, 128.4, 129.2, 132.9, 137.6, 139.0, 149.4; *m*/*z* (EI) 289 ($[M]^+$, 39%), 91 ($[C_6H_5CH_2]^+$, 100).

***N*-(2-Dihydroxyborylbenzyl)-*N*-methyl-*m*-tolylamine (12)**

N-(2-Bromobenzyl)-*N*-methyl-*m*-tolylamine (5.00 g, 17.2 mmol) was mixed in distilled tetrahydrofuran (40 ml) under argon. The solution was cooled to −78 °C and then *n*-butyllithium (10.3 ml, 2.5 M in THF, 25.8 mmol, 1.5 equiv.) was syringed slowly into the reaction mixture. After stirring at −78 °C for 1 hour, the lithiated solution was transferred dropwise, using a canula, into dry THF (40 ml) containing trimethylborate (8.9 g, 86.0 mmol, 5 equiv.) at −78 °C under argon. The reaction was allowed to warm to room temperature before adding hydrochloric acid (40 ml, 1 M). After stirring for 1 hour, water (50 ml) was added and the resulting aqueous layer washed with hexane (2 × 50 ml) and salted with sodium chloride. The aqueous phase was extracted with dichloromethane (3 × 50 ml) and the organic layers combined, dried over $MgSO_4$ and filtered. The solvent was removed *in vacuo* and **12** (1.08 g, 25%) was afforded by precipitation from chloroform with hexane as a white solid (HRMS: Found 256.1501; $C_{15}H_{19}BNO_2$ requires 256.1509); mp 61–63 °C (dec.); δ_H(300 MHz; CD_3OD; Me_4Si) 2.41 (3 H, s, Ar–CH_3), 3.28 (3 H, s, Ar–CH_3), 4.90 (2 H, s, ArCH_2–NHAr), 7.26–7.49 (8 H, m, Ar-*H*); δ_C(125 MHz; CD_3OD; Me_4Si) 22.0, 45.7, 66.3, 120.3, 123.6, 131.0, 131.8, 132.1, 132.7, 134.4, 136.2, 137.2, 142.9, 143.3; *m*/*z* (ESI) 256 ($[MH]^+$, 100%).

***N*-(2-Dihydroxyborylbenzyl)-*N*-methyl-[3-methyl-4-(4-nitrophenylazo)phenyl]amine (13)**

4-Nitroaniline (0.05 g, 0.39 mmol) was mixed in water (1 ml), methanol (1 ml) and hydrochloric acid (1 ml, 10.0 M) and then cooled to 0–5 °C on an ice-bath. A chilled solution of sodium nitrite (0.03 g, 0.43 mmol, 0.2 M) was added dropwise. Excess nitrite was destroyed by the addition of sulfamic acid. *N*-(2-Dihydroxyborylbenzyl)-*N*-methyl-*m*-tolylamine (0.10 g, 0.39 mmol) was dissolved in methanol (2 ml) and dilute hydrochloric acid (1 ml, 1 M), then added dropwise to the reaction mixture, which quickly turned a red colour. Sodium acetate was added to raise the pH of the solution to 4 and this was then left to stir at 0–5 °C for 3 hours. Sodium hydroxide (1 M) was slowly added to raise the pH to 7. The resulting precipitate was collected by suction filtration and dried in a dessicator overnight to afford **13** (0.13 g, 82%) as a dark red solid (Found: C, 62.8; H, 5.2; N, 13.1. $C_{21}H_{21}BN_4O_4$ requires C, 62.4; H, 5.2; N, 13.8%) (HRMS: Found 405.1739, $[MH]^+$. $C_{21}H_{21}BN_4O_4$ requires 405.1734); mp 115–120 °C (dec.); λ_{max}(pH 8.21, 0.01 mol dm^{-3} KCl, 0.002752 mol dm^{-3} KH_2PO_4, 0.002757 mol dm^{-3} Na_2HPO_4, 52.1% MeOH: 47.9% H_2O w/w)/nm 501 (ε/dm^3 mol^{-1} cm^{-1} 29300); ν_{max}(KBr disk)/cm^{-1} 1599 (N=N), 1512 and 1333 (NO_2); δ_H(300 MHz; CD_3OD; Me_4Si) 2.68 (3 H, s, Ar–CH_3), 3.11 (3 H, s, Ar-CH_3), 4.66 (2 H, s, ArCH_2–NHAr),

6.72–6.79 (2 H, m, Ar–*H*), 7.19–7.40 (5 H, m, Ar–*H*), 7.70–7.76 (1 H, m, Ar–*H*), 7.91 (2 H, d, *J* 12.0, Ar–*H*), 8.32 (2 H, d, *J* 12.0, Ar–*H*); δ_C(125 MHz; CD_3OD; Me_4Si) 18.5, 40.2, 58.3, 113.0, 115.4, 118.3, 123.5, 125.7, 127.7, 127.9, 128.9, 130.1, 133.0, 142.8, 143.9, 148.8, 155.5, 158.1; *m*/*z* (ESI) 405 ($[MH]^+$, 100%).

N-Benzyl-*m*-tolylamine (14)

Benzaldehyde (1.04 g, 9.84 mmol) and *m*-toluidine (1.05 g, 9.84 mmol) were mixed in toluene (50 ml) and heated at reflux for 15 hours in a Dean–Stark apparatus. After cooling, the solvent was removed *in vacuo* to afford a yellow oil, which was used directly in the next reaction step without further purification. Sodium borohydride (0.74 g, 19.7 mmol) was added in small portions to a stirred solution of the imine from the previous step in methanol (40 ml) at room temperature. TLC showed completion of the reaction after 2 hours. The reaction mixture was poured on to ice (5 g) and concentrated hydrochloric acid (1 ml) and stirred for 30 minutes, before removing most of the solvent *in vacuo*. Water (30 ml) was added and then the aqueous layer was extracted with dichloromethane. The organic extracts were combined, dried ($MgSO_4$) and filtered. The solvent was removed *in vacuo* to yield **14** (1.87 g, 96%) as a brown oil (HRMS: Found 197.1197. $C_{14}H_{15}N$ requires 197.1205); δ_H(300 MHz; $CDCl_3$; Me_4Si) 2.37 (3 H, s, Ar–C*H*$_3$), 4.04 (1 H, br s, N*H*), 4.39 (2 H, s, ArC*H*2–NHAr), 6.49–6.70 (3 H, m, Ar–*H*), 7.16 (1 H, t, *J* 6.0, Ar–*H*), 7.33–7.50 (4 H, m, Ar–*H*); δ_C(75 MHz; $CDCl_3$; Me_4Si) 21.7, 48.3, 109.9, 113.7, 118.5, 127.18, 127.5, 128.6, 129.2, 139.0, 139.6, 148.2; *m*/*z* (EI) 197 ($[M]^+$, 60%), 91 ($[C_6H_5CH_2]^+$, 100).

N-Benzyl-*N*-[3-methyl-4-(4-nitrophenylazo)phenyl]amine (15)

The procedure to form **6** was repeated using benzyl-*m*-tolylamine (0.20 g, 1.01 mmol) instead of *N*-(2-dihydroxyborylbenzyl)-*m*-tolylamine (all other reagents were used in the same mole ratios). Precipitation from chloroform with hexane afforded analytically pure **15** (0.08 g, 23%) as a dark red solid (Found: C, 69.1; H, 5.4; N, 16.3. $C_{20}H_{18}N_4O_2$ requires C, 69.3; H 5.2; N, 16.2%); mp 147–149 °C (dec.); ν_{max}(KBr)/cm^{-1} 1604 (N=N), 1507 and 1328 (NO_2); δ_H(300 MHz; $CDCl_3$; Me_4Si) 2.67 (3 H, m, Ar–C*H*$_3$), 4.43 (2 H, d, *J* 6.0, ArC*H*$_2$–NHAr), 4.71 (1 H, t, *J* 6.0, N*H*), 6.47–6.55 (2 H, m, Ar–*H*), 7.25–7.38 (5 H, m, Ar–*H*), 7.73–7.78 (1 H, m, Ar–*H*), 7.86–7.92 (2 H, m, Ar–*H*), 8.27–8.33 (2 H, m, Ar-*H*); δ_C(75 MHz; $CDCl_3$; Me_4Si) 18.3, 47.90, 111.5, 113.3, 117.9, 122.9, 124.9, 127.7, 127.9, 129.1, 138.3, 143.4, 143.7, 147.5, 152.2, 157.2; *m*/*z* (EI) 346 ($[M]^+$, 42%), 196 ($[M - N_2C_6H_4NO_2]^+$, 38), 91 ($[C_6H_5CH_2]^+$, 100).

Absorption–pH titration of 6, 7, 8, 9, 10 and 13

The UV–visible absorption spectra of **6** (5.66×10^{-5} mol dm^{-3}), **7** (4.66×10^{-5} mol dm^{-3}), **8** (5.47×10^{-5} mol dm^{-3}), **9** (7.33×10^{-5} mol dm^{-3}) and **10** (5.34×10^{-5} mol dm^{-3}) in a 0.05 mol dm^{-3} NaCl 33% methanol: 67% water (w/w) solution, were all recorded as the pH was changed from pH 2 to 12 in approximate intervals of 0.5 pH units. The pH was controlled using minimum volumes of sodium hydroxide and hydrochloric acid solutions. The same experiment was repeated with **13** (1.86×10^{-5} mol dm^{-3}) in a 0.05 mol dm^{-3} NaCl 67% methanol: 33% water (w/w) solution.

Absorption–pH titrations of 6, 7, 8, 9, 10 and 13 in the presence of D-fructose

The previous experiment was repeated with the addition of 0.05 mol dm^{-3} D-fructose to the solution in all cases.

Absorption–saccharide titrations of 6, 7, 8, 9, 10 and 13 at pH 11.32

The UV–visible absorption spectra of **6** (2.83×10^{-5} mol dm^{-3}), **7** (3.26×10^{-5} mol dm^{-3}), **8** (2.74×10^{-5} mol dm^{-3}), **9** (5.86×10^{-5} mol dm^{-3}), **10** (4.27×10^{-5} mol dm^{-3}) and **13** (2.09×10^{-5} mol dm^{-3}) in a pH 11.32 buffer (0.01000 mol dm^{-3} KCl, 0.002771 mol dm^{-3} $NaHCO_3$, 0.002771 mol dm^{-3} Na_2CO_3 in 52.1 wt% methanol: 47.9 wt% water),[23] were recorded as increasing amounts of various saccharides were added to the solution.

Absorption–saccharide titrations of 6 and 13 at pH 8.21

The UV–visible absorption spectra of **6** (2.83×10^{-5} mol dm^{-3}) and **13** (2.00×10^{-5} mol dm^{-3}) in a pH 8.21 buffer (0.01000 mol dm^{-3} KCl, 0.002752 mol dm^{-3} $KHPO_4$, 0.002757 mol dm^{-3} Na_2HPO_4 in 52.1 wt% methanol: 47.9 wt% water),[23] were recorded as increasing amounts of various saccharides were added to the solution.

Acknowledgements

T. D. J. wishes to acknowledge the Royal Society, the EPSRC, and Beckman-Coulter for support. C. J. W. wishes to acknowledge the EPSRC and Avecia Limited for support through the award of a Studentship. We would also like to acknowledge the support of the University of Bath.

References

1 J. H. Hartley, T. D. James and C. J. Ward, *J. Chem. Soc., Perkin Trans. 1*, 2000, 3155.
2 A. P. Davis and R. S. Wareham, *Angew. Chem., Int. Ed.*, 1999, **38**, 2978.
3 T. D. James, K. R. A. S. Sandanayake and S. Shinkai, *Angew. Chem., Int. Ed. Engl.*, 1996, **35**, 1911.
4 J. P. Lorand and J. O. Edwards, *J. Org. Chem.*, 1959, **24**, 769.
5 T. D. James, K. R. A. S. Sandanayake and S. Shinkai, *Supramol. Chem.*, 1995, **6**, 141.
6 T. D. James, P. Linnane and S. Shinkai, *Chem. Commun.*, 1996, 281.
7 H. R. Snyder and C. Weaver, *J. Am. Chem. Soc.*, 1948, **70**, 232.
8 H. S. Snyder and S. L. Meisel, *J. Am. Chem. Soc.*, 1948, **70**, 774.
9 H. Gilman, L. Santucci, D. R. Swayampi and R. O. Ranck, *J. Am. Chem. Soc.*, 1957, **79**, 2898.
10 N. Nagasaki, H. Shinmori and S. Shinkai, *Tetrahedron Lett.*, 1994, **35**, 2201.
11 M. Takeuchi, M. Taguchi, H. Shinmori and S. Shinkai, *Bull. Chem. Soc. Jpn.*, 1996, **69**, 2613.
12 C. J. Davis, P. T. Lewis, M. E. McCarroll, M. W. Read, R. Cueto and R. M. Strongin, *Org. Lett.*, 1999, **1**, 331.
13 K. R. A. S. Sandanayake and S. Shinkai, *J. Chem. Soc., Chem. Commun.*, 1994, 1083.
14 G. Wulff, *Pure Appl. Chem.*, 1982, **54**, 2093.
15 H. Shinmori, M. Takeuchi and S. Shinkai, *J. Chem. Soc., Perkin Trans. 2*, 1998, 847.
16 K. Koumoto and S. Shinkai, *Chem. Lett.*, 2000, 856.
17 K. Koumoto, M. Takeuchi and S. Shinkai, *Supramol. Chem.*, 1998, **9**, 203.
18 P. Gordon and P. Gregory, *Organic Chemistry in Colour*, Springer-Verlag, 1987.
19 H. Zollinger, *Color Chemistry*, VCH, Weinheim, 1991.
20 C. S. De Ligny and M. Rehbach, *Recl. Trav. Chim. Pays-Bas*, 1960, **79**, 727.
21 B. Valeur, J. Pouget, J. Bourson, M. Kaschke and N. P. Ernsting, *J. Phys. Chem.*, 1992, **96**, 6545.
22 C. R. Cooper and T. D. James, *J. Chem. Soc., Perkin Trans. 1*, 2000, 963.
23 D. D. Perrin and B. Dempsey, *Buffers for pH and Metal Ion Control*, Chapman & Hall, 1974.
24 J. H. Hartley and T. D. James, *Tetrahedron Lett.*, 1999, **40**, 2597.
25 *Advances in Linear Free Energy Relationships*, eds. N. B. Chapman & J. Shorter, Plenum Press, London, 1972.